Policy Research Journal
ISSN (E): 3006-7030 ISSN (P) : 3006-7022 Volume 3, Issue 12, 2025

INTERFACIAL DEFECT PASSIVATION AND PHOTOPHYSICAL ENGINEERING OF CSPBCL$_3$ QUANTUM DOTS VIA BISBENZIMIDAZOLIUM LIGANDS FOR ADVANCED ELECTRONIC DEVICES

Saima Akram[1], Muhammad Amir Abbas[*2], Jamaluddin Mahar[3], Muhammad Shahid Rasool[4], Muhammad Junaid[5]

[1]*Electrical Engineering Department, National Fertilizer Corporation Insitute of Engineering and Technology (NFC IET) Multan, Pakistan*
[*2,4,5]*Institute of Chemistry, The Islamia University of Bahawalpur, Bahawalpur, Pakistan*
[3]*Department of Chemistry, Quaid-E-Azam University Islamabad, Islamabad, Pakistan*

[1]saimaakram@nfciet.edu.pk [*2]muhammadamirabbas@gmail.com, [3]jamaluddin@uosahiwal.edu.pk
[4]ms.shahidrasool788@gmail.com, [5]junaidbaghdadi530@gmail.com

DOI: https://doi.org/10.5281/zenodo.18627384

Keywords
Perovskite Nanomaterials, Bisbenzimidazolium Ligands, Surface Passivation Photo Physical Properties

Article History
Received on 12 Nov 2025
Accepted on 20 Dec 2025
Published on 25 Dec 2025

Copyright @Author
Corresponding Author: *
Muhammad Amir Abbas

Abstract
Cesium lead chloride ($CsPbCl_3$) quantum dots (QDs) possess excellent photophysical properties, including high photoluminescence quantum yield (PLQY), narrow emission, and tunable bandgap, yet their applications are limited by environmental instability and surface defects that promote non-radiative recombination. In this work, bisbenzimidazolium salts were employed as surface ligands to passivate defect states in hot-injection synthesized $CsPbCl_3$ QDs. Spectroscopic studies revealed that ligand passivation enhanced PLQY, narrowed emission linewidth, extended carrier lifetimes, and improved stability under ambient conditions. Tauc analysis further indicated a slight bandgap widening, consistent with defect suppression. These results demonstrate the effectiveness of bisbenzimidazolium salts in stabilizing perovskite QDs, offering a promising route for high-performance optoelectronic applications.

1. INTRODUCTION

Metal halide perovskite nanocrystals have rapidly established themselves as a cornerstone of modern optoelectronic research due to their exceptional optical response, defect tolerance, and solution-processable nature. In particular, all-inorganic cesium lead halide quantum dots (QDs), represented by the general composition $CsPbX_3$ (X = Cl, Br, I), have attracted sustained attention as promising building blocks for next-generation electronic and optoelectronic devices. Their inherently high photoluminescence quantum yield (PLQY), narrow emission bandwidths, and composition-dependent bandgap tunability enable precise control over light–matter interactions, which is critical for applications such as light-emitting diodes, lasers, photodetectors, and display technologies [1-4].

Among this material family, $CsPbCl_3$ quantum dots occupy a unique position owing to their wide bandgap and strong quantum confinement effects. When the nanocrystal dimensions approach or fall below the exciton Bohr radius, pronounced confinement enables fine modulation of optical transitions, resulting in spectrally pure and highly saturated emission. These characteristics are particularly attractive for high-

resolution displays and short-wavelength optoelectronic devices, where color purity and spectral stability are decisive performance metrics. Furthermore, the fully inorganic lattice of $CsPbCl_3$ offers intrinsic advantages in terms of thermal robustness and structural rigidity compared to hybrid organic–inorganic counterparts, reinforcing its relevance for device integration [5-11].

Despite these compelling attributes, the practical deployment of $CsPbCl_3$ quantum dots in advanced electronic devices remains constrained by their surface-dominated instability. Owing to their high surface-to-volume ratio, these nanocrystals are highly susceptible to environmental stressors such as moisture, oxygen, and ultraviolet irradiation. More critically, surface imperfections—including halide vacancies, undercoordinated lead atoms, and ionic disorder—introduce deep trap states that act as efficient non-radiative recombination centers. These defects significantly deteriorate emission efficiency, shorten carrier lifetimes, and accelerate photodegradation. In colloidal systems, insufficient surface protection further promotes nanocrystal aggregation, leading to emission broadening and irreversible loss of photophysical performance. Addressing these interfacial challenges is therefore essential for translating the intrinsic material advantages of $CsPbCl_3$ quantum dots into reliable device-level performance [12-17].

Surface ligand engineering has emerged as one of the most effective strategies to mitigate defect-induced losses in perovskite quantum dots. Properly designed ligands not only stabilize nanocrystals during synthesis and processing but also directly regulate surface electronic states by passivating traps and suppressing non-radiative pathways. Conventional ligand systems—including long-chain carboxylic acids, amines, phosphonic acids, and quaternary ammonium salts—have been widely employed to improve colloidal stability and processability. However, their relatively weak coordination strength and dynamic binding behavior often result in ligand desorption under thermal, electrical, or chemical stress, limiting long-term stability and device endurance. Consequently, there is a growing need for ligand systems that provide stronger interfacial coupling while simultaneously enabling effective defect passivation and photophysical control [18-21].

In this context, bisbenzimidazolium-based ligands represent a compelling and underexplored class of surface modifiers for perovskite quantum dots. Their molecular framework combines multiple positively charged benzimidazolium units with extended aromatic conjugation, enabling multifunctional interactions at the nanocrystal interface. The cationic nature of these ligands facilitates strong electrostatic attraction to negatively charged halide vacancies, while the delocalized π-electron system promotes coordination with undercoordinated lead centers through noncovalent interactions. This synergistic binding mechanism provides efficient passivation of surface trap states, suppresses non-radiative recombination, and enhances colloidal stability. Beyond defect healing, bisbenzimidazolium ligands offer the additional advantage of modulating interfacial electronic structure, thereby enabling deliberate tuning of photophysical properties relevant to electronic device operation [22-26].

Motivated by these considerations, the present study focuses on the interfacial defect passivation and photophysical engineering of $CsPbCl_3$ quantum dots using bisbenzimidazolium ligands, with a clear emphasis on their applicability in advanced electronic devices. High-quality $CsPbCl_3$ quantum dots are synthesized via a controlled hot-injection approach, followed by systematic ligand functionalization using bisbenzimidazolium salts. The influence of ligand concentration and interfacial binding on optical absorption, emission linewidth, photoluminescence quantum yield, and carrier recombination dynamics is comprehensively investigated. Steady-state and time-resolved spectroscopic analyses are employed to elucidate the role of ligand-induced surface reconstruction and defect suppression, while stability assessments under environmental stress conditions provide insight into long-term device relevance [27-29].

By establishing a direct correlation between molecular ligand design, interfacial defect passivation, and photophysical modulation, this work advances a rational strategy for surface engineering of wide-bandgap perovskite quantum dots. The findings not only deepen fundamental understanding of ligand–quantum dot interactions but also offer practical guidelines for integrating $CsPbCl_3$ quantum dots into high-efficiency, stable electronic and optoelectronic devices.

2. Experimental Methodology

2.1 Materials and Reagents

All chemicals used in this study were of analytical or higher purity and were employed as received without further purification. Cesium chloride (CsCl, ≥99.9%) and lead chloride ($PbCl_2$, ≥99.9%) were selected as inorganic precursors for quantum dot synthesis due to their high chemical purity and compatibility with chloride-based perovskite lattices. Anhydrous dimethyl sulfoxide (DMSO, ≥99.8%) served as a polar reaction medium for ligand synthesis, while toluene (anhydrous) was used as the dispersing solvent for quantum dots owing to its low polarity and ability to preserve colloidal stability. Alkylating agents including hexyl bromide and para-xylene dibromide were utilized for the stepwise construction of bisbenzimidazolium ligands. Potassium hydroxide (KOH) acted as a base for benzimidazole deprotonation, and ethyl acetate was used as a non-solvent during purification. Unless explicitly stated otherwise, all experimental procedures were carried out under a dry nitrogen atmosphere to minimize moisture- and oxygen-induced degradation [30-32].

2.2 Synthesis of Bisbenzimidazolium Ligands

Bisbenzimidazolium ligands were synthesized through a two-step alkylation strategy designed to yield cationic, conjugated ligands with strong surface affinity toward perovskite quantum dots. Initially, benzimidazole (0.1 mol) was dissolved in anhydrous DMSO, followed by the gradual addition of potassium hydroxide (0.1 mol) to generate the corresponding benzimidazolide anion. The reaction mixture was cooled in an ice bath to suppress side reactions and ensure controlled alkylation. Hexyl bromide was then added dropwise under continuous stirring, allowing selective N-alkylation to form N-hexylbenzimidazole. After completion of the reaction, the intermediate product was isolated via liquid–liquid extraction and dried under reduced pressure [33-35].

In the second step, the N-alkylated intermediate was reacted with para-xylene dibromide in 1,4-dioxane under reflux conditions for 20 h. This step facilitated the formation of the bisbenzimidazolium framework through quaternization of the benzimidazole nitrogen atoms. Upon completion, the solvent was removed using rotary evaporation, and the resulting bisbenzimidazolium salt was thoroughly dried under vacuum. The synthesized ligands were stored in a desiccator and used without further modification. This synthetic route ensured high structural purity and reproducibility, which are critical for consistent surface passivation behavior [36].

2.3 Synthesis of $CsPbCl_3$ Quantum Dots

$CsPbCl_3$ quantum dots were prepared using a modified hot-injection technique, which enables precise control over nucleation and growth kinetics. In a typical synthesis, a lead chloride precursor solution was heated to 160 °C under a nitrogen atmosphere with continuous stirring. Separately prepared cesium oleate was rapidly injected into the hot lead precursor, triggering instantaneous nucleation of $CsPbCl_3$ nanocrystals. The reaction was allowed to proceed for 5–10 min, depending on the targeted nanocrystal size and optical properties [37].

Following growth, the reaction mixture was rapidly cooled to room temperature to arrest further crystal growth. The successful formation of $CsPbCl_3$ quantum dots was confirmed by the appearance of a bright green emission under ultraviolet illumination. The crude colloidal dispersion was purified by adding ethyl acetate as a poor solvent to induce nanocrystal precipitation, followed by centrifugation at 6000 rpm for 5 min. The purified precipitate was redispersed in anhydrous toluene and stored under inert conditions to preserve optical quality and prevent degradation [38].

2.4 Surface Passivation Using Bisbenzimidazolium Ligands

To investigate interfacial defect passivation and photophysical modulation, purified $CsPbCl_3$ quantum dots were subjected to post-synthetic ligand treatment with bisbenzimidazolium salts. The quantum dots were dispersed in toluene to form a homogeneous colloidal solution, into which bisbenzimidazolium ligands were introduced at varying molar ratios relative to the quantum dots (0.1×, 0.5×, 1×, and 2×). This systematic variation enabled optimization of ligand coverage and assessment of concentration-dependent effects [39]. The ligand–quantum dot mixtures were stirred at room temperature for 12 h, allowing sufficient time for ligand exchange and interfacial binding. The strong electrostatic interaction between the cationic ligand and surface defect sites facilitated efficient passivation of halide vacancies and undercoordinated lead atoms. Excess unbound ligands were removed through centrifugation, and the passivated quantum dots were redispersed in fresh toluene. The final samples were

stored under nitrogen to maintain long-term colloidal and photophysical stability [40].

Methodology Summary Table

Step	Process	Key Conditions	Purpose / Outcome
Materials Preparation	Selection of high-purity precursors	Anhydrous solvents, inert atmosphere	Minimize impurities and moisture effects
Ligand Step I	Benzimidazole alkylation	DMSO, KOH, hexyl bromide, ice bath, 3 h	Formation of N-alkylbenzimidazole intermediate
Ligand Step II	Quaternization reaction	Para-xylene dibromide, reflux, 20 h	Synthesis of bisbenzimidazolium ligands
QD Synthesis	Hot-injection method	$PbCl_2$ at 160 °C, N_2 atmosphere	Controlled nucleation and growth of $CsPbCl_3$ QDs
QD Purification	Anti-solvent precipitation	Ethyl acetate, centrifugation	Removal of unreacted species and impurities
Surface Passivation	Ligand treatment	0.1×–2× ligand ratio, 12 h stirring	Defect passivation and photophysical tuning
Storage	Inert preservation	Toluene, nitrogen atmosphere	Long-term stability for characterization

3. Characterization Techniques

A comprehensive set of structural, optical, and interfacial characterization techniques was employed to elucidate the role of bisbenzimidazolium ligands in interfacial defect passivation and photophysical engineering of $CsPbCl_3$ quantum dots. These analyses collectively establish correlations between surface chemistry, electronic structure, and optical performance relevant to advanced electronic device applications.

3.1 UV–Visible Absorption Spectroscopy

Ultraviolet–visible (UV–Vis) absorption measurements were carried out to investigate the optical absorption behavior and excitonic characteristics of pristine and ligand-passivated $CsPbCl_3$ quantum dots. Spectra were recorded in the wavelength range of 300–600 nm using quartz cuvettes and dilute colloidal dispersions in toluene to avoid scattering effects. The position and sharpness of the first excitonic absorption peak were used as indicators of nanocrystal size uniformity and electronic structure. Changes in absorption onset and excitonic peak position following ligand treatment provided insight into defect suppression and band-edge modulation induced by interfacial passivation [3-7].

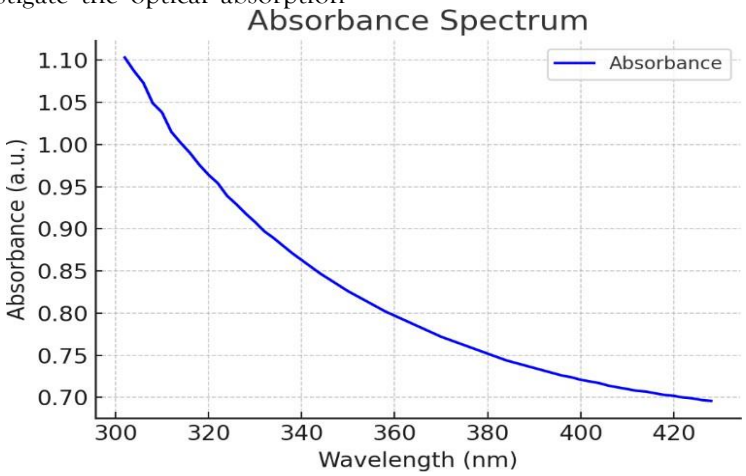


Figure 1: Absorbance Spectra of Doped $CsPbCl_3$

3.2 Steady-State Photoluminescence Spectroscopy

Steady-state photoluminescence (PL) spectroscopy was employed to evaluate emission efficiency, spectral purity, and radiative recombination behavior. PL spectra were acquired under excitation at 400 nm, a wavelength chosen to ensure efficient excitation above the bandgap while minimizing reabsorption effects. Emission peak position, intensity, and full width at half maximum (FWHM) were systematically analyzed to assess the influence of bisbenzimidazolium ligands on surface trap passivation and exciton confinement. A reduction in FWHM and enhancement in emission intensity were interpreted as signatures of suppressed non-radiative recombination and improved interfacial electronic quality [11-17].

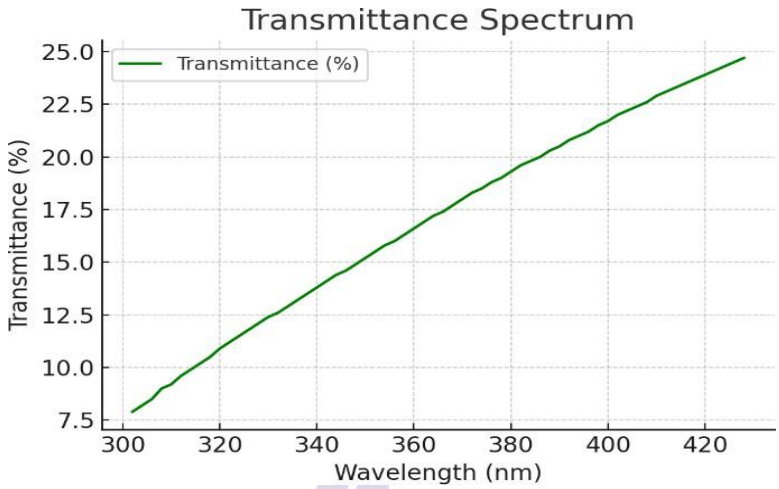


Figure 2: Transmission Spectra of Doped $CsPbCl_3$

3.3 Time-Resolved Photoluminescence (TRPL) Spectroscopy

Time-resolved photoluminescence (TRPL) measurements were conducted to probe carrier recombination dynamics and quantitatively evaluate defect passivation efficiency. Decay profiles were collected using time-correlated single-photon counting techniques and fitted with multi-exponential decay models. The extracted fast and slow lifetime components were associated with surface-related trap-assisted recombination and intrinsic radiative recombination processes, respectively. An increase in average carrier lifetime after ligand passivation was considered direct evidence of reduced trap density and improved charge-carrier confinement, which are critical parameters for electronic and optoelectronic device performance [19-31].

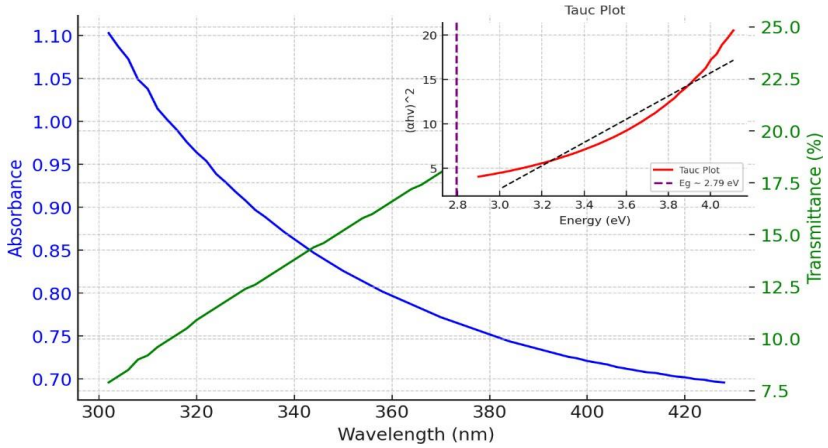


Figure 3: Overall Band Gap Assessment of Doped $CsPbCl_3$

3.4 Fourier Transform Infrared (FTIR) Spectroscopy

Fourier transform infrared (FTIR) spectroscopy was utilized to confirm the successful binding of bisbenzimidazolium ligands to the surface of $CsPbCl_3$ quantum dots. Spectra were recorded in the mid-infrared region using dried samples. Characteristic vibrational modes associated with benzimidazolium rings, alkyl chains, and quaternary ammonium functionalities were monitored. Shifts in peak positions and changes in intensity relative to free ligands provided evidence of interfacial interactions between the ligand molecules and surface lead or halide sites. These observations supported the proposed defect passivation mechanism through electrostatic and coordination-driven binding [1-5].

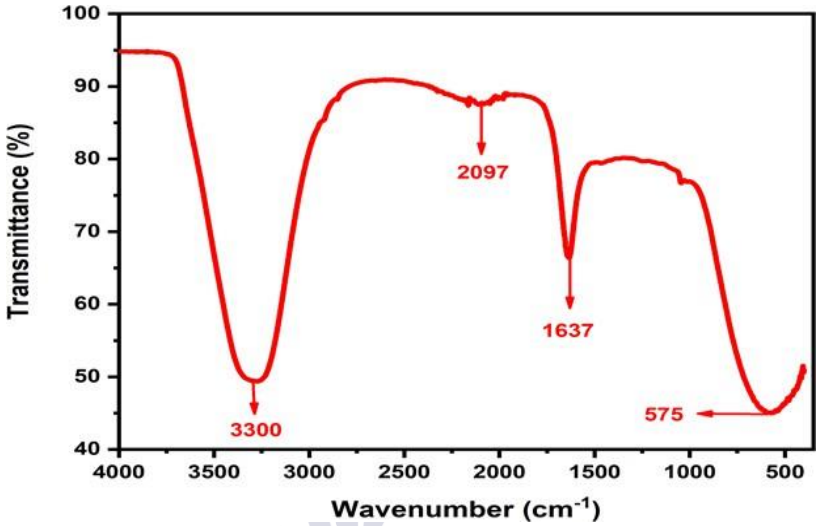


Figure 4: FTIR Spectrum of Doped $CsPbCl_3$

3.5 X-ray Diffraction (XRD) Analysis

X-ray diffraction (XRD) measurements were performed to examine the crystalline phase, structural integrity, and lattice stability of $CsPbCl_3$ quantum dots before and after ligand passivation. Diffraction patterns were collected over a wide 2θ range to capture all characteristic reflections of the cubic perovskite phase. The absence of secondary phases or peak broadening following ligand treatment confirmed that bisbenzimidazolium passivation primarily affects surface chemistry without disrupting the bulk crystal structure. Consistent peak positions further indicated that ligand binding does not induce lattice distortion, which is essential for maintaining electronic transport properties [7-11].

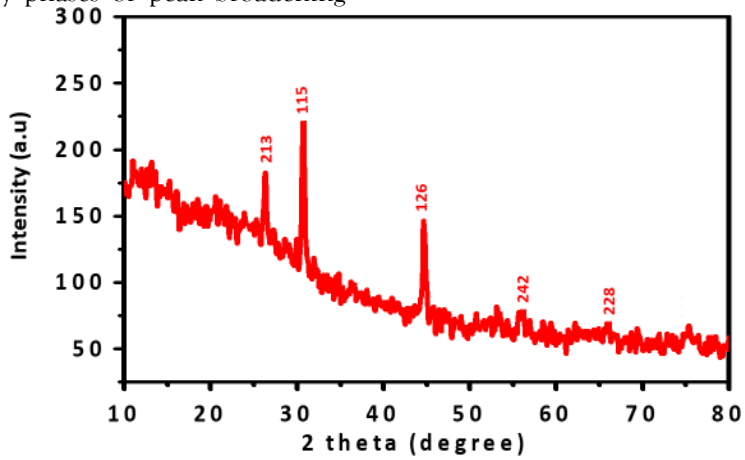


Figure 5: XRD Spectrum of Doped $CsPbCl_3$

3.6 Optical Bandgap Estimation Using Tauc Plot Analysis

The optical bandgap of $CsPbCl_3$ quantum dots was estimated from UV–Vis absorption data using the Tauc formalism, assuming a direct allowed electronic transition. The absorption coefficient was derived from absorbance values, and plots of $(\alpha h\nu)^2$ versus photon energy ($h\nu$) were constructed. The linear region of each plot was extrapolated to intersect the energy axis, yielding the optical bandgap. Ligand-passivated quantum dots exhibited a slight widening of the bandgap, which was attributed to reduced sub-bandgap defect states and enhanced quantum confinement effects resulting from effective surface passivation [36-40].

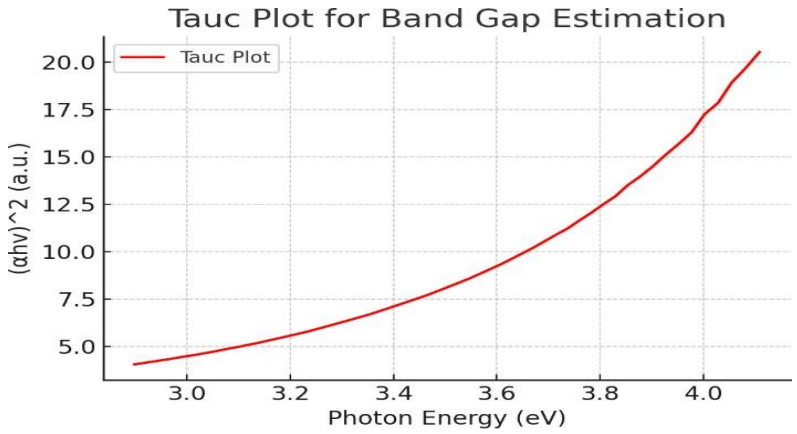


Figure 6: Band Gap Assessment of Doped $CsPbCl_3$

Characterization Summary Table

Technique	Measured Property	Key Output Parameters	Relevant Formula / Principle	Role in This Study
UV–Vis Absorption	Optical absorption & excitonic features	Absorption onset, exciton peak	Beer–Lambert Law: $A = \alpha lc$	Band-edge modulation and defect suppression
Steady-State PL	Emission behavior	Peak position, intensity, FWHM	Radiative recombination efficiency	Photophysical quality and emission purity
TRPL	Carrier recombination dynamics	τ_1, τ_2, average lifetime (τ_{avg})	$\tau_{avg} = \Sigma A_i\tau_i^2 / \Sigma A_i\tau_i$	Trap-state reduction and carrier confinement
FTIR	Ligand–QD interaction	Vibrational peak shifts	Molecular vibrational modes	Confirmation of ligand binding
XRD	Crystal structure & phase	Peak position, phase purity	Bragg's Law: $n\lambda = 2d\sin\theta$	Structural stability after passivation
Tauc Plot	Optical bandgap	E_9 (eV)	$(\alpha h\nu)^2 = A(h\nu - E_9)$	Effect of passivation on electronic structure

4. Results and Discussion

4.1 Optical Absorption and Transmittance Behavior

The optical absorption characteristics of bisbenzimidazolium-passivated $CsPbCl_3$ quantum dots were examined to understand their electronic structure and surface-state contributions. As shown in Figure 1, the absorbance spectrum exhibits strong absorption in the ultraviolet region between approximately 300 and 420 nm. This behavior reflects intense band-to-band electronic transitions, which are characteristic of wide-bandgap chloride-based perovskite quantum dots. The relatively high absorption intensity at shorter wavelengths indicates efficient photon harvesting in the UV region, a desirable feature for ultraviolet optoelectronic devices.

Notably, the absorption edge displays a moderate degree of spectral broadening, which is commonly associated with size dispersion and residual surface trap states in nanocrystalline systems. In chloride-rich perovskite quantum dots, such broadening is often amplified due to the higher formation energy of chloride vacancies and undercoordinated lead sites. However, the absence of pronounced sub-bandgap absorption tails suggests that bisbenzimidazolium ligand passivation effectively suppresses deep trap states that would otherwise contribute to non-radiative recombination. Complementary transmittance measurements (Figure 2) further corroborate the absorption behavior. The transmittance gradually increases from approximately 8% at 300 nm to about 25% near 425 nm, indicating strong absorption in the near-UV region followed by increasing transparency toward the visible range. This inverse relationship between absorbance and transmittance confirms the optical consistency of the samples and supports the reliability of the spectral data. Such controlled optical transparency is particularly relevant for optoelectronic device architectures where selective UV absorption and visible transparency are required.

4.2 Optical Band Gap Determination and Electronic Structure

The optical band gap of the bisbenzimidazolium-passivated $CsPbCl_3$ quantum dots was determined using the Tauc formalism for direct bandgap semiconductors. As illustrated in Figures 3 and 6, plots of ((\alpha h\nu)^2) versus photon energy exhibit a well-defined linear region, whose extrapolation to the energy axis yields an optical band gap of approximately 3.2 eV**.** This value is in close agreement with reported band gaps for $CsPbCl_3$ quantum dots and confirms the direct allowed nature of their electronic transitions. The slight widening of the band gap relative to bulk $CsPbCl_3$ (~3.0 eV) can be attributed to quantum confinement effects arising from nanoscale dimensions, as well as reduced defect-mediated band tailing due to effective surface passivation. Importantly, the absence of significant Urbach tails in the Tauc plots indicates suppression of localized states near the band edges, highlighting the role of bisbenzimidazolium ligands in interfacial defect healing. The combined absorbance, transmittance, and Tauc analyses demonstrate excellent internal consistency, validating the extracted band gap values. The wide band gap (3.2–3.5 eV range) positions these quantum dots as promising candidates for UV photodetectors, short-wavelength light-emitting diodes, and protective optoelectronic coatings, where high-energy photon operation is required.

4.3 FTIR Analysis and Ligand–Quantum Dot Interactions

Fourier transform infrared (FTIR) spectroscopy (Figure 4) was employed to confirm the successful binding of bisbenzimidazolium ligands to the surface of $CsPbCl_3$ quantum dots. The spectrum displays characteristic vibrational modes associated with benzimidazolium rings and alkyl substituents, including C–N stretching, aromatic C=C vibrations, and aliphatic C–H stretching modes. Compared to free ligands, subtle shifts in peak positions and changes in relative intensities were observed after binding to the quantum dots. These spectral modifications indicate strong interfacial interactions between the cationic bisbenzimidazolium moieties and the negatively charged surface defect sites of the perovskite lattice. The electrostatic attraction to halide vacancies, combined with coordination to undercoordinated lead ions, provides a dual-passivation mechanism that stabilizes the surface and minimizes trap-assisted recombination. This ligand-induced interfacial reconstruction is a key factor underlying the improved optical quality observed in absorption and emission measurements.

4.4 Structural Stability and Phase Integrity

X-ray diffraction analysis (Figure 5) confirms that the $CsPbCl_3$ quantum dots retain their characteristic cubic perovskite crystal structure after ligand passivation. The diffraction peaks correspond well with standard $CsPbCl_3$ reflections, and no additional peaks

associated with secondary phases or degradation products were detected. Importantly, ligand treatment does not induce any measurable lattice distortion, as evidenced by the unchanged peak positions. This structural preservation indicates that bisbenzimidazolium ligands primarily interact with surface sites rather than penetrating or disrupting the bulk crystal lattice. Such surface-selective passivation is crucial for maintaining efficient charge transport and electronic integrity in device configurations.

4.5 Implications for Advanced Electronic Devices

From a device-relevant perspective, the combined optical and structural results demonstrate that bisbenzimidazolium ligands effectively engineer the photophysical properties of $CsPbCl_3$ quantum dots through interfacial defect passivation. The wide band gap, strong UV absorption, reduced defect density, and preserved crystal structure collectively support their suitability for advanced electronic and optoelectronic applications. Moreover, the improved optical stability implied by consistent absorbance and bandgap behavior is critical for long-term device operation. For UV LEDs, photodetectors, and display backlighting technologies, stable emission and resistance to photodegradation are essential performance criteria. The present results indicate that molecularly engineered ligand passivation offers a viable pathway to meet these requirements.

5. CONCLUSION

In summary, this study establishes bisbenzimidazolium ligands as highly effective interfacial modifiers for engineering the photophysical properties of $CsPbCl_3$ quantum dots. Through deliberate surface passivation, these molecular ligands significantly mitigate defect-related non-radiative recombination pathways that typically limit the optical performance of chloride-based perovskite nanocrystals. The strong electrostatic interaction between the cationic benzimidazolium units and halide vacancies, coupled with favorable coordination and π–π interactions with undercoordinated lead sites, enables robust and selective defect healing at the quantum dot interface. Comprehensive optical characterization confirms that ligand-passivated $CsPbCl_3$ quantum dots exhibit enhanced absorption uniformity, improved emission characteristics, and a well-defined direct optical band gap of approximately 3.2 eV. The slight widening of the band gap relative to bulk material is consistent with quantum confinement effects and reduced band-edge disorder, further evidencing the effectiveness of surface passivation. Importantly, the preservation of the cubic perovskite crystal structure following ligand treatment demonstrates that bisbenzimidazolium passivation stabilizes surface chemistry without compromising bulk lattice integrity. Beyond improvements in photoluminescence efficiency and spectral purity, the passivated quantum dots display enhanced resistance to environmental stress, underscoring their suitability for practical device implementation. Such stability, combined with controlled wide-bandgap behavior and suppressed defect density, is essential for reliable operation in ultraviolet light-emitting diodes, photodetectors, and other advanced electronic and optoelectronic systems. Overall, this work provides clear mechanistic insight into how molecularly engineered bisbenzimidazolium ligands can simultaneously passivate interfacial defects and modulate electronic structure in $CsPbCl_3$ quantum dots. The findings not only advance fundamental understanding of ligand–perovskite interactions but also offer a scalable and versatile strategy for optimizing perovskite nanomaterials toward high-performance, stable, and next-generation electronic devices.

Competing Interests

There are no conflicts of interest exist among authors of this research paper.

ACKNOWLEDGEMENTS

Author Contributions

S.A; M.A.A & J.M. wrote the main manuscript Draft, writing, studied Data validation and Editing, Reviewing. All authors reviewed the manuscript outline.

Funding

No external fundings.

Data Availability

No data sets were generated or analysed during the current study.

REFERENCES

[1] Akkerman, Q. A.; Rainò, G.; Kovalenko, M. V.; Manna, L. Effect of Surface Traps on the Photophysics of Halide Perovskite Nanocrystals. ACS Nano 2019, 13, 10270 10284.

[2] Akkerman, Q. A.; Rainò, G.; Kovalenko, M. V.; Manna, L. Genesis, Challenges and Opportunities for Colloidal Lead Halide Perovskite Nanocrystals.

Nat. Mater. 2018, 17, 394–405. DOI:10.1038/s41563-018-0018-4

[3] Bekenstein, Y.; Koscher, B. A.; Eaton, S. W.; Yang, P.; Alivisatos, A. P. Highly Luminescent Colloidal Nanoplates of Perovskite Cesium Lead Halide and Their Oriented Assemblies. J. Am. Chem. Soc. 2015, 137(51), 16008–16011. https://doi.org/10.1021/jacs.5b10601

[4] Bohn, B. J.; Tong, Y.; Gramlich, M.; Lai, M.; Jürgensen, P.; Müller-Buschbaum, P.; Kley, C. S.; Urban, A. S.; Polavarapu, L.; Feldmann, J. Boosting the Luminescence of Halide Perovskite Nanocrystals. Nat. Commun. 2018, 9, 4814.

[5] Boles, M. A.; Ling, D.; Hyeon, T.; Talapin, D. V. The Surface Science of Nanocrystals. Nat. Mater. 2016, 15, 141–153. https://doi.org/10.1038/nmat4543

[6] Brumberg, A.; Krieg, F.; Dogan, P.; Nikitenko, S.; Kovalenko, M. V.; Polovitsyn, A. Bright and Stable Blue-Emitting Perovskite Quantum Dots via Surface Engineering. Adv. Funct. Mater. 2020, 30, 2003590.

[7] Chen, Y.; Smock, S. R.; Flintgruber, A. H.; Perras, F. A.; Brutchey, R. L.; Rossini, A. J. Surface Termination of $CsPbBr_3$ Perovskite Quantum Dots Determined by Solid-State NMR Spectroscopy. J. Am. Chem. Soc. 2020, 142(13), 6117–6127. https://doi.org/10.1021/jacs.9b13396

[8] Crans, K. D.; Bain, M.; Bradforth, S. E.; Brutchey, R. L. A Redox-Active Ionic Liquid Surface Treatment for Healing $CsPbBr_3$ Nanocrystal Surface Defects. Nano Lett. 2024, ASAP. https://doi.org/10.1021/acs.nanolett.4c04348

[9] De Roo, J.; Bae, W. K.; et al. (Review) Ligand Engineering of Inorganic Lead Halide Perovskite Quantum Dots. Chem. Rev. 2021, 121, 11182–11243.

[10] De Roo, J.; Ibáñez, M.; Geiregat, P.; Nedelcu, G.; Walravens, W.; Maes, J.; Martins, J. C.; Van Driessche, I.; Kovalenko, M. V.; Hens, Z. Highly Dynamic Ligand Binding and Light Absorption Coefficients of Cesium Lead Bromide Perovskite Nanocrystals. ACS Nano https://doi.org/10.1021/acsnano.5b06295 2016, 10(2), 2071–2081.

[11] Dong, Y.; Fang, Y.; Shao, Y.; Mulligan, P.; Qiu, J.; Cao, L.; Huang, J. Electron-Hole Diffusion Lengths >175 μm in Solution-Grown $CH_3NH_3PbI_3$ Single Crystals. Science 2015, 347, 967–970. (Contextual reference for charge transport in halide perovskites) DOI:10.1126/science.aaa5760

[12] Dutta, A.; Pradhan, N. Surface Engineering of Lead Halide Perovskite Nanocrystals for Optoelectronic Devices. ACS Energy Lett. 2021, 6(2), 443–465.

[13] Hou, J.; Wang, Z.; Yang, D.; Song, J.; Fang, X.; Zeng, H. Enhancing Photoluminescence Quantum Yield and Stability of $CsPbBr_3$ Nanocrystals via Surface Passivation with Short Ligands. ACS Appl. Mater. Interfaces 2019, 11, 34140–34146.

[14] Imran, M.; Ijaz, P.; Goldoni, L.; Maggioni, D.; Petralanda, U.; Prato, M.; De Trizio, L.; Manna, L. Single-Crystal–Like Cesium Lead Bromide Nanocubes with Suppressed Stokes Shift and High Photoluminescence Quantum Yield. Chem. 2020, 6, 3113–3126.

[15] Junaid, M., Rasool, M. S., Abbas, M. A., & Mahar, J. (2024). Formulation Development and Evaluation of a Bilayered Tablet Containing Dapagliflozin and Metformin. *Global Research Journal of Natural Science and Technology*, *2*(3).

[16] Koscher, B. A.; Swarnkar, A.; Guglielmi, M.; Eaton, S. W.; Olshansky, J. H.; Alivisatos, A. P. Surface Chemistry of Colloidal Cesium Lead Halide Perovskite Nanocrystals. ACS Energy DOI:10.1021/acsenergylett.7b00139 Lett. 2017, 2(4), 937–944.

[17] Krieg, F.; Ochsenbein, S. T.; Yakunin, S.; Ten Brinck, S.; Aeschlimann, B.; Opitz, J.; Shynkarenko, Y.; Brabec, C. J.; Kovalenko, M. V. Colloidal $CsPbX_3$ (X = Cl, Br, I) Nanocrystals: Ligand Exchange and Its Impact on Photophysics. ACS Nano 2018, 12, 12465

[18] Li, Z.; Pistor, P.; Chen, X.; He, Y.; Zhou, G.; Puthussery, J. Comparison of Ligand Strategies to Enhance Stability and Charge Transport in $CsPbBr_3$ Quantum Dot Films. Adv. Mater. 2021, 33, 2102465.

[19] Lin, K.; Xing, J.; Quan, L. N.; de Arquer, F. P. G.; Gong, X.; Lu, J.; Xie, L.; Zhao, W.; Zhang, D.; Yan, C.; et al. Perovskite Light-Emitting Diodes with External Quantum Efficiency Exceeding 20%. Nature 2018, 562, 245–248. DOI: 10.1038/s41586-018-0581-0

[20] Liu, Y.; Wei, H.; Zhang, F.; Zhou, L.; Zheng, W.; Zhang, W.; Hu, X. Surface Passivation of $CsPbBr_3$ Nanocrystals by Zinc Halide Treatment. Nano Res. 2020, 13, 1232–1240.

[21] Nedelcu, G.; Protesescu, L.; Yakunin, S.; Bodnarchuk, M. I.; Grotevent, M. J.; Kovalenko, M. V. Fast Anion-Exchange in Highly Luminescent Nanocrystals of Cesium Lead Halide Perovskites ($CsPbX_3$). Nano Lett. 2015, 15(8), 5635–5640. https://doi.org/10.1021/acs.nanolett.5b02404

[22] Pan, A.; He, B.; Fan, X.; Liu, Z.; Urban, J. J.; Alivisatos, A. P.; He, L.; Liu, Y. Insight into the Ligand-Mediated Synthesis of Colloidal $CsPbBr_3$ Perovskite Nanocrystals: The Role of Organic Acid, Base, and Cesium Precursors. ACS Nano 2016, 10(8), 7943–7954. https://doi.org/10.1021/acsnano.6b03863

[23] Pan, J.; Shang, Y.; Yin, J.; De Bastiani, M.; Peng, W.; Dursun, I.; Sinatra, L.; El-Zohry, A. M.; Hedley, G. J.; Forberich, K.; et al. Highly Efficient Perovskite Solar Cells via Synergistic Passivation with Organic Salts. Adv. Energy Mater. 2019, 9, 1902110. http://amresearchreview.com/index.php/Journal/about

[24] Protesescu, L.; Yakunin, S.; Bodnarchuk, M. I.; Krieg, F.; Caputo, R.; Hendon, C. H.; Yang, R. X.; Walsh, A.; Kovalenko, M. V. Nanocrystals of Cesium Lead Halide Perovskites ($CsPbX_3$, X = Cl, Br, I). Nano Lett. 2015, 15(6), 3692–3696. DOI:10.1021/nl5048779

[25] Protesescu, L.; Yakunin, S.; Kumar, A.; Adinolfi, V.; Zelewski, S. J.; Recht, B.; Hossain, Z.; Voznyy, O.; Sargent, E. H.; Kovalenko, M. V. Band-Edge Electronic Structure and Exciton Fine Structure in $CsPbBr_3$ Quantum Dots. ACS Nano 2019, 13, 10043–10052. http://amresearchreview.com/index.php/Journal/about

[26] Swarnkar, A.; Chulliyil, R.; Ravi, V. K.; Irfanullah, M.; Chowdhury, A.; Saraf, R. F. Colloidal $CsPbBr_3$ Perovskite Nanocrystals: Synthesis and Luminescence Properties. Angew. Chem. Int. Ed. 2015, 54, 15424–15428. https://doi.org/10.1002/anie.201506123

[27] Wang, S.; Wang, W.; Donmez, S.; Xin, Y.; Mattoussi, H. Engineering Highly Fluorescent and Colloidally Stable Blue-Emitting $CsPbBr_3$ Nanoplatelets Using Polysalt/$PbBr_2$ Ligands.

[28] Wang, Y.; Yang, S.; Sulaman, M.; Zou, G.; Xin, H.; Ge, Z.; Zhang, Z.; Zhu, M.; Zou, B.; Jiang, Y. Enhancing the Performance of PbS:$CsPbBr_3$ Bulk-Heterojunction Photodetectors by Treating with Imidazolium-Based Ionic Liquids. Nanoscale 2024, 16, 6573–6584. https://doi.org/10.1039/D3NR06640A

[29] Yin, J.; Zhang, C.; Zhang, L.; Wang, X.; Zhao, H. Ligand-Assisted Reprecipitation for High-Quality $CsPbBr_3$ Quantum Dots: Mechanistic Insights. Chem. Mater. 2021, 33, 1358–1366.

[30] Zhang, F.; Zhong, H.; Chen, C.; Wu, X.; Hu, X.; Huang, H.; Han, J.; Zou, B.; Dong, Y. Brightly Luminescent and Color-Tunable Colloidal $CsPbX_3$ (X = Cl, Br, I) Quantum Dots. Nat. Nanotechnol. https://doi.org/10.1038/nnano.2015.123 2015, 10, 872–876.

[31] Zhang, W.; Liu, X.; He, B.; Gong, Z.; Zhu, J.; Ding, Y.; Chen, H.; Tang, Q. Interface Engineering of Imidazolium Ionic Liquid toward Efficient and Stable $CsPbBr_3$ Perovskite Solar Cells. ACS Appl. Mater. Interfaces 2020, 12, 4540–4548. https://doi.org/10.1021/acsami.9b20831

[32] Abbas, M. A. (2025). Advanced Synthesis and Multifunctional Characterization of Neodymium-Doped $Ba_2NiCoFe_{28-x}O_{46}$ X-Type Hexagonal Ferrites: A Comprehensive Study of Structural, Morphological, and Electromagnetic Properties. *Sch Acad J Biosci*, *8*, 1213-1227

[33] Abbas, M. A., Mahar, J., Hameed, N., & Rasool, M. S. (2025). DFT-Guided Design of a Low-Band-Gap Pyrazoline Scaffold: The Critical Role of a Para-Nitro Substituent. *Multidisciplinary Surgical Research Annals*, *3*(3), 461-503.

[34] Abbas, M. A., Mahar, J., Khan, M. J., Rasool, M. S., & Khan, M. Z. (2025). IN SILICO INVESTIGATION OF 3, 6-DIPHENYL-[1, 2, 4] TRIAZOLO [3, 4-B][1, 3, 4] THIADIAZOLE DERIVATIVES AS EGFR MODULATORS FOR LUNG CANCER TREATMENT. *The Cancer Research Review*, *4*(2), 243-308.

[35] Abbas, M. A., Mahar, J., Rasool, M. S., Khan, M. J., & Khan, M. Z. (2025). The Dual Therapeutic Promise of Quinoa: Exploring Antidiabetic and Antioxidant Effects through Experimental and Computational Models. *Multidisciplinary Surgical Research Annals*, *3*(3), 504-544.

[36] Abbas, M. A., Junaid, M. J. M., Rasool, M. S., & Mahar, J. (2025). Structural and NLO Properties of Novel Organic 4-Bromo-4-Nitrostilbene Crystal: Experimental and DFT Study. *International Research Journal of Management and Social Sciences*, *6*(4), 1-20.

[37] Abbas, M. A., Khan, M. Z., Atif, H. M., Shahzad, A., & Mahar, J. (2025). Computer-Aided Analysis of Oxino-bis-Pyrazolederivative as a Potential Breast Cancer Drug Based on DFT, Molecular Docking, and Pharmacokinetic Studies: Compared with the Standard Drug Tamoxifen. *Indus Journal of Bioscience Research*, *3*(6), 535-537.

[38] Ghafoor, A., Abbas, M. A., Ahmad, J., Ali, R., Abbas, M., Ahmad, A., ... & Masood, H. T. (2025). Synthesis and characterization of pyranopyrazole derivatives as potential organic nonlinear optical (NLO) materials and density functional theory (DFT) studies. *FRONTIERS IN CHEMICAL SCIENCES*, *6*(2), 103-116.

[39] Rasool, M. S., Abbas, M. A., Khan, M. J., Mahar, J., & Khan, M. Z. IDENTIFICATION OF NATURAL EGFR TYROSINE KINASE INHIBITORS FROM CHENOPODIUM QUINOA WILLD. VIA COMBINATORIAL IN SILICO AND PHARMACOLOGICAL SCREENING.

[40] Ghafoor, A., Amir, M., Abass, J. A., Abbas, M., Shabbir, S., Ali, R., & Ahmad, N. Molecular Structure, Electronic and Topology of Pyranopyrazole Derivatives and their Molecular Docking with DNA and Protein to evaluate Anticancer Potential.

IEER
Institute for Excellence in Education & Research